Available online at www.sciencedirect.com
ScienceDirect
Polymer 48 (2007) 849–859
polymer
www.elsevier.com/locate/polymer

Electrically conductive carbon black (CB) filled in situ microfibrillar poly(ethylene terephthalate) (PET)/polyethylene (PE) composite with a selective CB distribution

Kun Dai, Xiang-Bin Xu, Zhong-Ming Li*

College of Polymer Science and Engineering, State Key Laboratory of Polymer Materials Engineering, Sichuan University, Chengdu, Sichuan 610065, People's Republic of China

Received 29 July 2006; received in revised form 30 November 2006; accepted 13 December 2006
Available online 20 December 2006

Abstract

In the present study, it was attempted to fabricate a new conductive carbon black (CB) filled poly(ethylene terephthalate) (PET)/polyethylene (PE) in situ microfibrillar composite with a lower percolation threshold through selectively localizing CB particles in the surfaces of the PET microfibrils. The CB particles were first mixed with PE matrix, and then PET was added into CB/PE compound. Subsequently, the CB/PET/PE composite was subjected to a slit die extrusion, hot stretch and quenching process to generate in situ PET microfibrils, in which CB particles moved to the surfaces of the PET microfibrils simultaneously. The morphological observation showed that the PET phases formed well-defined microfibrils, and CB particles did overwhelmingly localize in the surfaces of the PET microfibrils, which led to a very low percolation threshold, i.e., 3.8 vol%, and a good conductivity. The conductive network was built by the contact and overlapping of the CB particles coated PET microfibrils. In addition, the CB particles remaining in the PE matrix also contributed to the conductive paths, especially for the high CB loading filled microfibrillar composites. Because of the complexity of the distribution of CB particles, a high critical resistance exponent t ($t = 6.4$) exists in this conductive composite. To reveal the possibility of the migration of CB particles from PE to PET, the morphology of the CB/PET/PE composite mixed for different times was examined. It was found that, depending on the mixing time, the CB particles gradually migrated from the PE matrix to the surfaces at first, and then to the center of the PET phases. The preferable distribution of CB particles was originated from several factors including interfacial tension, viscosity, molecule polarity, and mixing process. Furthermore, during the mixing process of the CB/PET/PE composite, the migration of CB particles to PET phase from PE matrix led to the increase of both the viscosity ratio of the dispersed phase to the matrix and the volume of the dispersed phases, thus resulting in larger dispersed CB/PET composite phase particles.

Keywords: Carbon black; Electronically conductive composite; In situ microfibrillar blend

1. Introduction

Conductive polymer composites (CPC) based on insulating polymer matrix and electrically conductive fillers such as carbon black (CB), carbon nanotubes, graphite, metal powders, etc. [1–11] exhibit many interesting features due to their resistivity change with mechanical, thermal, electrical or chemical solicitations [12–15]. This versatility of CPC is the foundation for their applications such as self-regulated heating, positive temperature coefficient (PTC) materials, electromagnetic shielding, and chemical vapor detection, etc. [9,13,16,17]. For CB filled CPC, their properties usually depend on the features of both polymers (such as degree of crystallinity, melt viscosity, surface tension) and CB (such as species, surface area, chemical groups, and dibutyl phthalate (DBP) absorption values) [18–21]. While for a certain sort of CB, the distribution of CB particles in the material, as well as the interaction between CB and polymers, to a great degree, affects many properties of the CPC significantly, especially, the percolation threshold.

* Corresponding author. Fax: +86 28 8540 5324.
E-mail address: zm_li@263.net.cn (Z.-M. Li).

0032-3861/$ - see front matter © 2006 Elsevier Ltd. All rights reserved.
doi:10.1016/j.polymer.2006.12.026

Percolation threshold is the critical amount of CB to build originally continuous conductive networks, at which the drastic insulator–conductor transition appears. Reduction of the percolation threshold of CPC is of significance in lowering cost, easier processing and better mechanical properties. Therefore, it is a long-term major topic to investigate how to control the percolation threshold efficiently [18–20].

Up to now, there have been many investigations about controlling the percolation threshold by manipulating the distribution of CB particles, such as multi-percolation [22], segregated distribution [18,20,23], and electrical field-induced method, etc. [24]. Multi-percolation can be achieved by locating CB particles in one phase of a continuous multi-phase blend selectively, and the percolation threshold of CPC can be reduced greatly [22]. By preferentially blending CB into a high-density polyethylene (HDPE) matrix, Foulger prepared CB filled co-continuous poly(ethylene-*co*-vinyl acetate) (EVA)/HDPE composite with CB particles selectively localizing in EVA phase, and obtained a percolation threshold between 3.6 and 4.2 wt% [25]. Narkis et al. studied injection-molded polypropylene (PP)/GF (glass fiber)/CB-based composite, the morphologies of which were characterized by a continuum of insulating GF becoming conducting as a result of being encapsulated with the polyamide (PA) minor component and localization of the CB particles mostly at the PP/PA interfaces. They claimed that a triple-percolation has been achieved in this composite with less than 2 wt% CB [26]. Another approach to reduce percolation threshold is that CB particles were distributed at the interfaces of multi-phase polymeric materials preferentially [1]. By this approach, Gubbels et al. prepared an electrically conductive CB/polystyrene (PS)/PE composite, whose percolation threshold was surprisingly declined to ca. 0.4 wt%, being one of the lowest percolation values reported in the open literature by far [27,28]. Segregated distribution of CB particles in CPC can also lessen the percolation threshold remarkably. Zhang et al. fabricated a binary CB/waterborne polyurethane CPC by segregating dispersion of CB through in situ latex blending, and obtained a percolation threshold of 0.2 vol% [23]. Furthermore, the high voltage electric field was employed to control CB distribution so as to reduce percolation concentration [14,24]. As the applied electric field strength was 600 V/cm, the electric field-induced agglomeration of CB particles in epoxy resin led to a percolation network with only 0.12 vol% CB loading [29].

Nevertheless, every approach about reducing the percolation threshold of CPC has its more or less limitations. For example, the CPC obtained by a multi-percolation method usually have poor mechanical properties because of weak interfacial adhesion between immiscible polymer components. Therefore, it is still a tough challenge for reduction in the percolation threshold of CPC in less sacrifice of their combination properties.

In our previous studies [30–34], CB particles were first localized in the minor phase (polyethylene terephthalate, PET), and then the conductive CB/PET masterbatch was in situ elongated to form conductive in situ microfibrils in polyethylene (PE) matrix during melt extrusion processing. After compression molding, a fine conductive three-dimensional microfibrillar network was constructed, thus resulting in a relatively low percolation threshold (6.0 vol%). For this CPC, both the positive temperature coefficient (PTC) effect and the surface structure of the microfibrils were directly related to the maximum packing fraction Φ_{max} of the CB particles in the PET microfibrils [34]. When the CB loading is below the maximum packing fraction Φ_{max}, the CB/PET microfibrils cannot conduct well in the composite, because there was a layer of nearly pure polymer in the surfaces of microfibrils. When the CB loading is beyond the maximum packing fraction Φ_{max}, CB particles could migrate to the surfaces of the microfibrils and a fine electrical network was built. To reach the Φ_{max}, a high CB loading must be added into the PET microfibrils. Most of the CB particles only served to cram the microfibrils and thus made the CB particles migrate to the surfaces of the microfibrils. In fact, these CB particles were nearly useless for the conductivity of the composites. This case indicates that the percolation of the in situ microfibrillar CB/PET/PE composite can be further reduced by manipulating the distribution of the CB. Based on this, if the conductive fillers are mainly, even totally localized in the surface region of the microfibrils rather than their inside, the conductive network can be more efficiently constructed, thus leading to a lower percolation threshold, and a higher conductivity. Apparently, to realize this structure design, the impact of the maximum packing fraction should be overcome, since it is a switch to decide whether the conductive fillers can lie in the surfaces of the microfibrils.

In the present paper, the influence of the maximum packing fraction Φ_{max} is attempted to eliminate by localizing CB particles in the surfaces of in situ microfibrils using the following procedures: (1) the CB particles were first mixed with PE matrix, and then PET was added into CB/PE compound; (2) the CB/PET/PE composite was subsequently subjected to a slit die extrusion, hot stretch and quenching process. Upon the designed processing operations, the CB particles can move towards the surfaces of the PET domains due to their more highly selective distribution in PET than in PE. To verify whether the CB particles can successfully migrate from PE to PET, the morphology of the CB/PET/PE composite mixed for different times was first examined in detail.

2. Experimental

2.1. Materials

The main materials used in this work are electrically conductive CB, PET and PE. The CB is VXC-605 with a DBP value of 148 ± 15 cm^3/100 g, purchased from Cabot Co. Ltd. The CB was dried at 120 °C for 10 h to get rid of the water before use. The PET was friendly donated by LuoYang Petroleum Chemical Co., LuoYang, China, which is a commercial grade of textile polyester with a number average molecular weight of ca. 2.3×10^4 g/mol. PE is a commercial high-density PE (Model 5000S) of DaQing Petroleum Chemical Co., Daqing, China, with a melt flow rate of 0.9 g/10 min at 190 °C, exerting a load of 21.6 N.

2.2. Migration of CB particles from PE matrix to PET phase

In order to examine the possibility of the migration for CB particles from PE matrix to PET phase, an experiment was performed as below: PE was first plasticized for 5 min in an internal mixer, then CB particles were added and mixed for 2 min, finally the PET chips were added to mix for 30 s, 60 s, 300 s, 600 s. The apparent shear rate is ca. 19.1 s^{-1}. The mixing temperature was fixed at 280 °C.

To get more information about the possibility of the migration of CB particles, CB/PET/PE composites were mixed in a Haake internal mixer for 20 min. Neat PET/PE blend was mixed by the same processing for comparison. The shear rate is 19.1 s^{-1}. The torque, which is the reflection of the viscosity, was recorded to check the migration process of CB particles.

2.3. Preparation of in situ microfibrillar CB/PET/PE composite

PE was first fed into an internal mixer and held for 5 min at 180 °C, and then CB particles were added and mixed at the same temperature for 5 min. The CB/PE masterbatch was granulated and dry mixed with PET chips. The mixture obtained was extruded through a slit die in a single-screw extruder. The temperature profile was 190, 250, 275 and 270 °C, from the hopper to the exit. The extrudate was hot stretched at a line speed of ca. 1.1 m/min by a take-up device with two pinching rolls to form the microfibrils [30–34]. After hot stretching, the extrudate was immediately quenched in a cold water (20 °C) bath. The ribbon with a thickness of about 0.2 mm was thus obtained. Subsequently, the ribbon was pelletized, and then compression molded into $10 \times 10 \times 2$ mm^3 board at 150 °C (the processing temperature of PE) for 10 min with a pressure of ca. 10 MPa. All the sheets were cooled to room temperature by cold compression molding for 5 min. Due to the high melting point of PET (about 257 °C), the in situ PET microfibrils can be successfully reserved in the composite during molding.

For comparison purpose, common CB/PE composites and CB/PET/PE composites without elongation were also prepared. The processes were the same as the microfibrillar CB/PET/PE composite except the extrusion temperature of common CB/PE CPC, which was set at the processing temperature of PE (from the hopper to the exit, the temperature was 100, 150, 200 and 200 °C).

For the sake of brevity, the hot stretched composite with in situ PET microfibrils is hereafter referred to as i-CB/PET/PE composite, and the directly mixed CB/PET/PE composite without hot stretch as d-CB/PET/PE composite. In the experiment of examining the migration of CB particles, unless it is specially pointed out, the mixing time is referred to the time that was used to mix just after PET was added.

2.4. Electrical property testing

When the volume resistivity of the samples is below 10^6 Ω cm, the volume electrical resistivity was measured by a four-probe method (ASTM D-991) using two multimeters and a voltage supply. The four-probe method can effectively avoid the contact resistance which affects the precision of the measurement. When the volume resistivity is relatively low, this method has adequate preciseness. A high resistivity meter was used when the volume resistivity of the samples is beyond 10^6 Ω cm. The sample dimensions for low and high resistivity measurements were $2 \times 10 \times 100$ mm^3 and $2 \times 100 \times 100$ mm^3, respectively.

2.5. Morphological observation

The specimens were fractured after frozen in liquid nitrogen for 1 h. The fracture surfaces were covered with a layer of gold to make them conductive, and then observed with a JEOL JSM-5900LV scanning electron microscope (SEM). For clear observation of the dispersed phase morphology, some specimens were immersed in hot xylene at about 125 °C for 15 h to dissolve the PE matrix away.

3. Results and discussion

3.1. Prediction for selective distribution of CB particles

For the origin of the heterogeneous distribution of conductive fillers in an immiscible polymer blend, Wu et al. recently claimed that the entropy penalty might play a main role in the movement of electrically conductive fillers [35]. However, it is still widely accepted to use Young's equation to predict the selective distribution of CB in a polymer composite, which was first suggested by Sumita et al. [36], and then was successfully used to prepare CB/PP/poly(methyl methacrylate) (PMMA) CPC [1]. The Young's equation is:

$$\gamma_{CB-\alpha} + \gamma_{\alpha-\beta} \cos\theta = \gamma_{CB-\beta} \tag{1}$$

$$w_a = \frac{\gamma_{CB-\beta} - \gamma_{CB-\alpha}}{\gamma_{\alpha-\beta}} \tag{2}$$

where θ is the contact angle of the polymer on the CB, w_a is the wetting coefficient, $\gamma_{CB-\alpha}$, $\gamma_{CB-\beta}$, and $\gamma_{\alpha-\beta}$ are the interfacial tension between CB and α-polymer, between CB and β-polymer, and between α- and β-polymer, respectively. If $w_a > 0$, that is, $\gamma_{CB-\beta} > \gamma_{CB-\alpha}$, CB particles will distribute overwhelmingly in α-polymer or at the interface, and if $w_a < 0$, that is, $\gamma_{CB-\beta} < \gamma_{CB-\alpha}$, CB particles will distribute in β-polymer or at the interfaces.

According to the literature [37], the interfacial tensions between CB and PET and between CB and PE are 5.9 mN/m and 13.1 mN/m, respectively. Hence, a very high probability exists that CB is better adhered to PET than to PE, or the larger affinity characterizing the CB/PET system due to the lower interfacial tension between CB and PET.

On the other hand, Chan et al. found that CB particles prefer to selectively locate in the lower melt viscosity phase in a multi-phase blend, regardless of the interfacial tension [38]. The minimization of the dissipative energy for absorption

of the fillers during shearing can explain this phenomenon [39]. For CB/PET/PE composite, the apparent viscosity at the melt mixing temperature (270 °C) and at a shear rate of 230.4 s^{-1} is 3.5 and 705.2 Pa s for PET and PE, respectively. CB particles, therefore, have stronger tendency to locate in PET than PE from the view of the thermodynamics.

The fact that there are many functional polar groups like carboxylic, phenolic, lactonic on the surface of CB is also a factor affecting the selective distribution of CB particles [40]. If the interactions between one polar polymer component and CB particles are strong enough, the interactions will influence the dispersion of CB particles [20,23,41–43]. As to CB/PET/PE composite, PET has a very high surface tension and polarity, while the PE is a nonpolar polymer. The interaction between PET phase and CB particles is, thus, stronger than that between PE phase and CB particles. In other words, CB particles have a priority to locate in the PET phase.

In this study, the special mixing procedures were designed to locate CB particles in the surfaces of PET phases. CB particles were firstly mixed with PE, and during the extrusion and hot stretching, there was sufficient time for CB particles to migrate from PE matrix to PET phase under shear flow.

The analyses above indicate that all these factors affecting the distribution of CB particles in a immiscible blend, including interfacial tension, viscosity, chemical groups on the surface of CB particles and the processing order, are in favor of the migration of the CB particles from PE matrix to dispersed PET phases.

3.2. Migration of CB particles in PET/PE blend

In order to probe how the migration of CB particles from PE matrix to the surfaces of PET microfibrils takes place, the morphology of CB, PET and PE mixture mixed for different times was observed as shown in Fig. 1 through Fig. 4.

The SEM micrographs of cryofractured surfaces for CB/PET/PE composite mixed for 30 s after the incorporation of PET are shown in Fig. 1. A typical incompatible morphology appears in which the interfaces are very clear and no evidence implies any adhesion. Taking into account the composition of the ternary composite, apparently, PE serves as the continuous phase, while the smaller spherical domains belong to PET phase. The diameter of PET particles is mainly 1–5 μm.

At early stage, due to limited mixing time (30 s), the CB particles (Fig. 1(a) and (b)) basically locate in the PE phase. In other words, the particles still did not migrate from PE phase into the PET phase at all. But their surfaces become rather coarse, possibly resulting from the scratch of the CB particles in the PE matrix.

With increasing the mixing time to 60 s (Fig. 2(a)–(c)), most PET particles still remain almost spherical (Fig. 2(a)), but their size becomes larger than that in Fig. 1(a). In addition, some particles appear in ellipsoid or rod.

To elucidate the structure inside the PET domains, a fractured PET particle was particularly observed at a high magnification as shown in Fig. 2(b) and (c), which corresponds to the outer and inner regions, respectively. Apparently, CB particles had successfully migrated to the outer region of PET particles (Fig. 2(b)), thus demonstrating the validity of above prediction for CB particle's selective distribution [19].

For the morphological evolution of dispersed melt droplets, there are two opposite processes taking place during mixing: breakup (upon continuous breakdown of the dispersed PET droplets) vs. coalescence (involving combination of the dispersed PET droplets that approach one another) [18,44,45]. The present case is more complicated due to the incorporation of CB particles. Continuous migration of CB particles to PET phase affects the volume fraction and the viscosity of the dispersed phase to the matrix phase. That is, for the dispersed phase (CB/PET), both its volume fraction and viscosity increases, while for the matrix phase (CB/PE), both its volume fraction and viscosity decreases. Consequently, migration of CB particles led to a higher volume ratio as well as a larger viscosity ratio of the dispersed phase to the continuous phase. Both factors have a positive effect on coarsening of the dispersed phase particles [18], so the increase of the dispersed PET phase size is reasonable.

Furthermore, it is interesting that the CB particles in Fig. 2(b) appear as tiny spheres rather than aggregates, while those in the matrix still as aggregates (Fig. 2(b)). The CB spheres in the PET phase are ca. 50 nm in diameter, which should be the primary particles [40,46]. This means that the

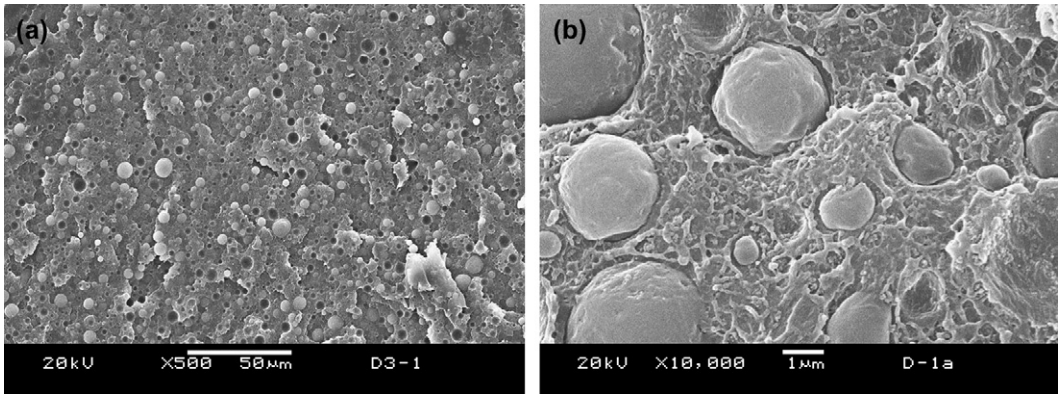

Fig. 1. SEM micrographs of the cryofractured surface of directly mixed CB/PET/PE composite with low and high magnifications. The mixing time is 30 s. The volume ratio of PET and PE is 1:3.2, and the CB loading is 3.5 vol%.

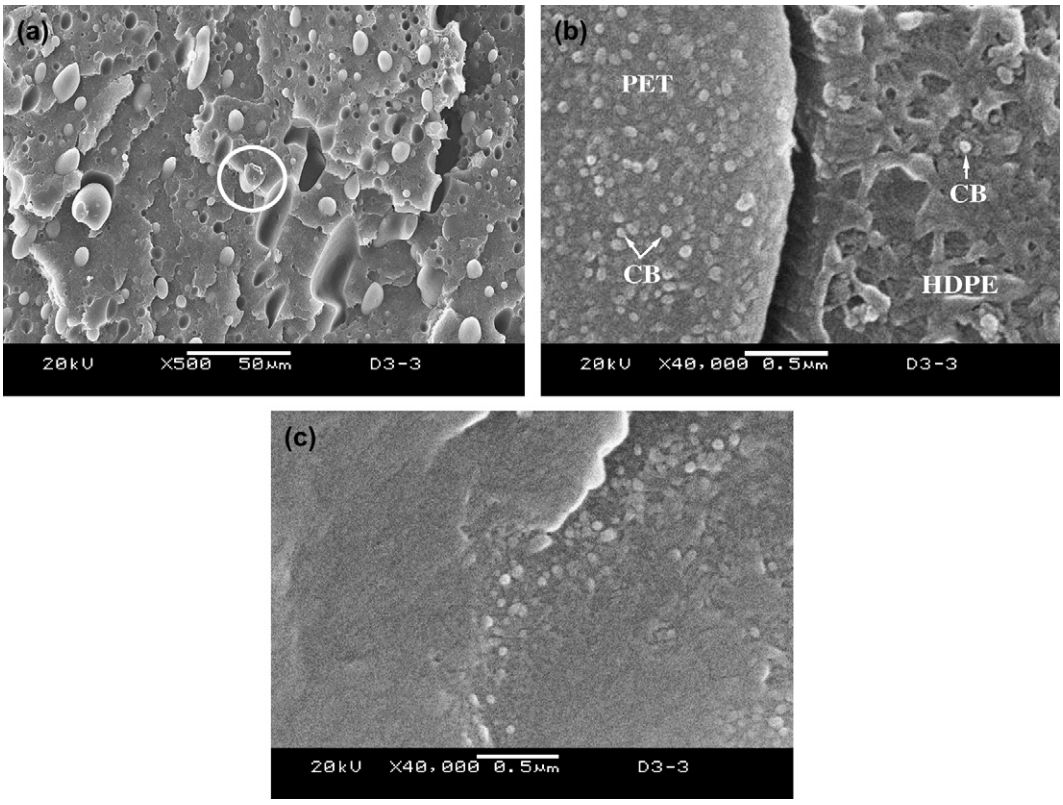

Fig. 2. SEM micrographs of the cryofractured surface of directly mixed CB/PET/PE composite with low and high magnifications. The mixing time is 60 s. The volume ratio of PET and PE is 1:3.2, and the CB loading is 3.5 vol%.

breakup and cleavage of the CB aggregates occurred to produce the original CB particles during their migration to PET phase. Presumably, there are the following possible reasons: (1) during drastic shear and elongational flow, some original particles were flaked off from their host aggregates, (2) these flaked primary particles had higher possibility to enter the PET phase due to their smaller size and higher affinity between CB and PET than between CB and PE [20,35–43]. Furthermore, there are still nearly no CB particles in the inner region of PET domains (Fig. 2(c)). This can be easily understandable because CB particles have no sufficient time to move entad.

Fig. 3 shows the cryofractured surface of CB/PET/PE composite with a mixing time of 300 s. The morphology of the PET phase is more complex, with a quite wide size distribution. The PET particles reduced greatly in number, and most of them remained in the same size, being similar with those in Fig. 2. It is surprising that some other PET particles became unexpectedly large and irregular upon shear mixing. The higher viscosity of the dispersed droplets upon CB addition affected the final morphology [47]. Because the continuous migration of CB particles to dispersed PET particles made the viscosity of PET phase to rise, resulting in a much higher dispersed phase/matrix viscosity ratio. The droplets would, therefore, be hard to breakup, at most, some of which were elongated, as shown in Fig. 3(a).

The detailed structural information inside the PET particles is shown in Fig. 3(b) and (c). Fig. 3(b) shows the interface between a dispersed PET phase and the PE matrix. The distribution of CB particles in the PET surface was also uniform under this condition. Fig. 3(c) shows the inner region of the PET particle. From this image, one can find that the CB particles have arrived at the center of the PET domain, though their distribution was not yet uniform.

Fig. 4(a)–(c) illustrates the cryofractured surface of CB/PET/PE composite mixed for 600 s. Fig. 4(b) displays the distribution of CB particles in the interface between the cryofractured PET phase and the PE matrix, while Fig. 4(c) shows the central region of the fractured PET particles. It is observed that CB particles were homogeneously distributed throughout the PET particles, PET particles become more irregular, and some of them are also unexpectedly large after a long time of mixing.

The migration of CB particles from PE matrix to PET phase should be reflected from the rheological properties since the phase structure and morphology influence the flow behavior of a blend. To demonstrate this point, CB/PET/PE composite was melt mixed in a Haake internal mixer, and the torque was recorded during mixing. Fig. 5 presents the torque as a function of mixing time for CB/PET/PE composite and PET/PE blend. The torque decreased sharply in the beginning for both neat PET/PE and CB/PET/PE, as a result of the melting of PE. The PET started to melt after about 1 min. At this moment, PET was in the form of large spherical drops in both neat PET/PE and CB/PET/PE. For neat PET/PE, the torque decreases slightly after about 4 min, indicating the completion of PET melting. With the increase of mixing time, the large spherical

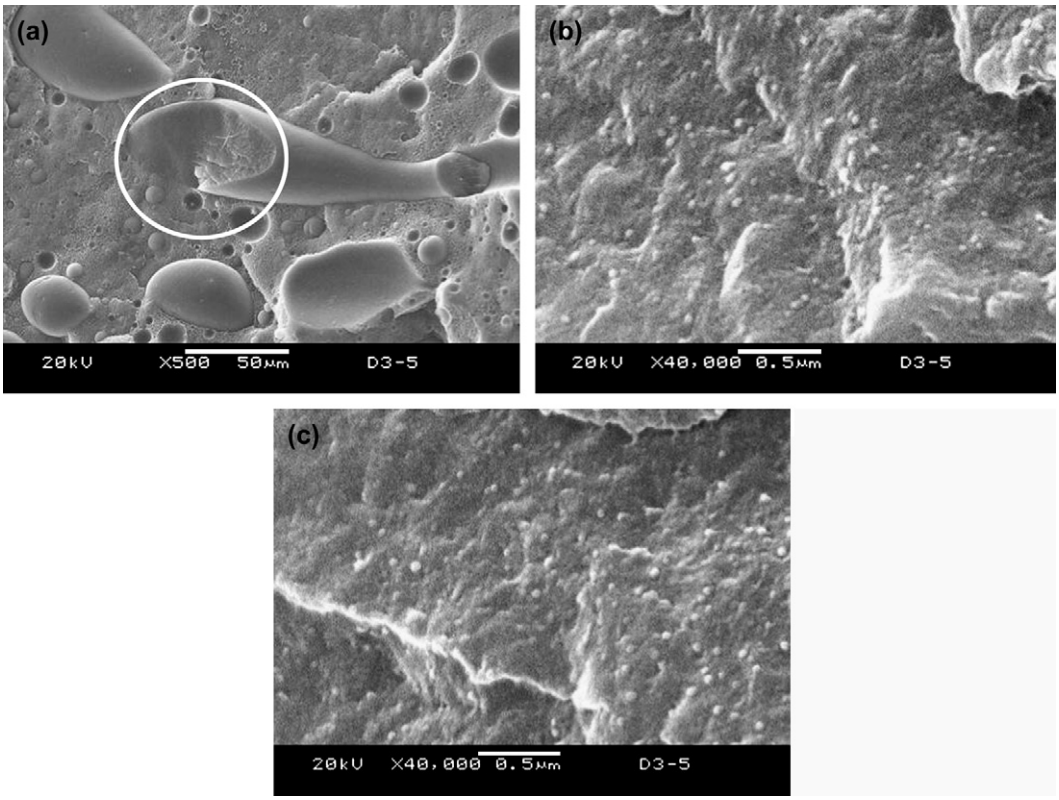

Fig. 3. SEM micrographs of the cryofractured surface of directly mixed CB/PET/PE composite with low and high magnifications. The mixing time is 300 s. The volume ratio of PET and PE is 1:3.2, and the CB loading is 3.5 vol%.

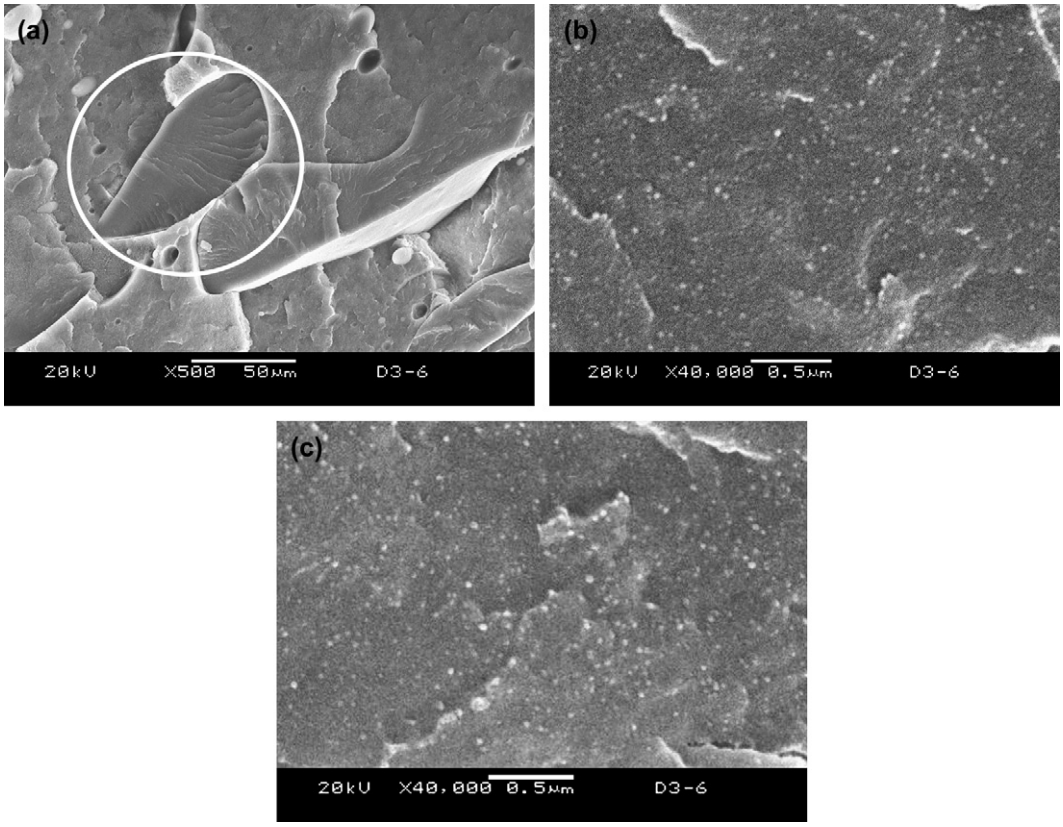

Fig. 4. SEM micrographs of the cryofractured surface of directly mixed CB/PET/PE composite with low and high magnifications. The mixing time is 600 s. The volume ratio of PET and PE is 1:3.2, and the CB loading is 3.5 vol%.

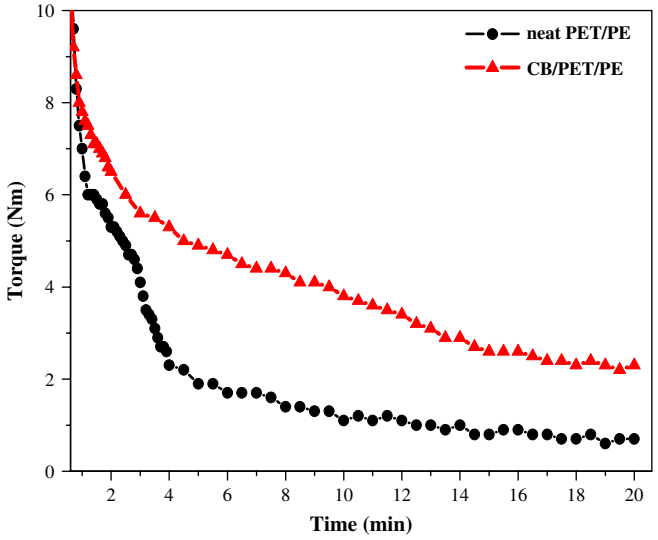

Fig. 5. Torque–time relationship for neat PET/PE and CB/PET/PE at 280 °C. The volume ratio of PET and PE for these two samples is 1:3.2. The CB loading in the CB/PET/PE is 3.5 vol%.

PET drops could be elongated to liquid fibers, and then broken into smaller droplets, so that the torque continued to decrease. Notwithstanding, some droplets simultaneously merged again. Finally, an equilibrium appears after about 8 min as a result of the dynamic processes of breakup and coalescence of the droplets [18,19]. Consequently, the torque remains constant.

But for CB/PET/PE composite, the case is quite different after the melting of PET particles. Large melted PET droplets surrounded with CB particles would also be elongated and broken into smaller ones, while it followed the gradual migration of CB particles to PET droplets. Therefore, the torque changed gently and the time needed for achieving the equilibrium became longer.

3.3. Morphology of in situ microfibrillar i-CB/PET/PE composite

From the above theoretical analysis and experimental observation from Fig. 1 to Fig. 5, it can be concluded that CB particles can successfully migrate from PE matrix to PET phase. That is, during shear mixing of CB/PET/PE composite, in which CB particles are initially localized in PE phase, CB particles will gradually move to the surface of PET domains, and then towards their center. As a result of this, it is feasible to fabricate an in situ microfibrillar CB/PET/PE composite with CB particles being accumulated at the surface regions of PET microfibrils using the slit die extrusion–hot stretching–quenching technique.

During this processing, the crystallization of both PE and PET would happen with decreasing temperature, which would also influence the localization and migration of CB. It is known that PE and PET both are semi-crystalline polymers. But PE has a higher crystallinity than PET, and the crystallization onset temperature of PET is much higher than that of PE [48,49]. Moreover, for CB particles, they can only reside in the amorphous regions of a polymer, and should be rejected from the crystalline regions [46]. Therefore, during the processing, PET phases would crystallize first. Since PET has a low crystallinity, the localization of CB particles distributed in PET microfibrils' surfaces would be hardly altered by the crystallization of PET. The crystallization of PE occurred later at about 120 °C and CB particles around the interfaces would be rejected from PE crystalline regions due to the high crystallinity of PE, and CB particles would be further accumulated at the interfaces. The crystallization of both PE and PET would be in favor of the selective localization of CB accordingly.

Fig. 6 shows the typical morphology of in situ microfibrillar i-CB/PET/PE composite fractured perpendicular to the stretch direction. In the fracture surface perpendicular to the flow direction, the section and the end of the PET microfibrils can be observed. It is very interesting that a lot of CB particles are accumulated in the surfaces of the PET microfibrils. In contrast, there are nearly no CB particles in the center of the PET microfibrils. This observation indicates that our structure design of the conductive composite has been successfully realized. This unique structure is in favor of the transfer of electrons between microfibrils contacted with each other, and thus the conductivity will undoubtedly be enhanced. The clusters appearing in the fracture surface that have quite rough surfaces are the ends of PET microfibrils. It indicates that CB particles stack throughout the surface of the microfibrils rather

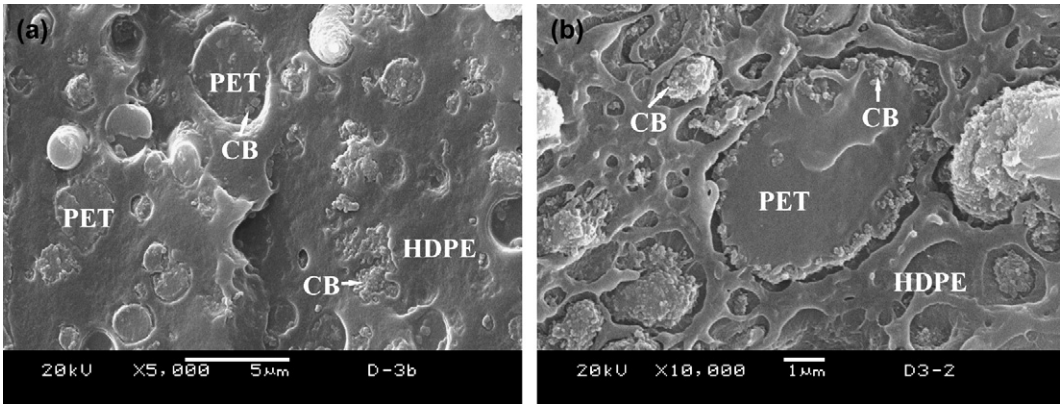

Fig. 6. SEM micrographs of the cryofractured surfaces of in situ microfibrillar i-CB/PET/PE composite with selectively locating CB in the surfaces of the PET microfibrils. The volume ratio of PET and PE is 1:3.2, and the CB loading is 3.5 vol%.

than only in their side surface. In addition, no obvious CB aggregates can be seen in the PE matrix, implying the efficient migration of CB particles to PET phase.

However, with the decreasing temperature, voids between PET microfibrils and PE matrix would be generated because of the poor interfacial adhesion between them (Fig. 6). This phenomenon is common in immiscible conductive composites and some carbon fibers filled conductive composites [50,51]. These voids would be bad for the mechanical properties of the CPC, but it would supply space for migration of CB particles [50], and these CB particles could also facilitate the construction of a fine conductive network. This effect on the localization of CB particles would fade away gradually with decreasing temperature.

Fig. 7 shows the representative morphology of the in situ microfibrillar i-CB/PET/PE composite. For clear observation, the PE matrix was dissolved away by hot xylene. During hot stretching through two pinching rolls, the melted PET droplets were elongated into liquid microfibrils, and subsequently, the extrudate was quenched by cold water to freeze the microfibrils. Fig. 7 indicates that the well-defined PET microfibrils were generated in situ by this extrusion–hot stretching–quenching process. The microfibrils' diameter is about 1–5 μm, which changes little with increasing the CB loading, while their length is hard to estimate due to the limited observed region. The particles on the surfaces of the microfibrils were CB, which, once again, demonstrates that the tailored morphology has been achieved through the present processing technique.

Fig. 8 shows the SEM micrographs of the morphology of in situ microfibrillar i-CB/PET/PE composite with a higher CB content, 8.1 vol%. It is found that some CB particles, even aggregates, were embedded in the surfaces of the PET microfibrils.

The SEM micrograph of the i-CB/PET/PE microfibrillar composite with 4.93 vol% CB is shown in Fig. 9 (note the magnification is not the same as Fig. 6(b)). The micrograph focused on the CB particles in the matrix near the PET phase. One can see that in the PE matrix, the CB aggregates increase with the CB loading compared to Fig. 6.

With the increasing CB loading, the distribution of CB particles became un-uniform and the morphology of the matrix changed greatly (Figs. 6 and 9). The main reason is that particles in the interfaces will reject the entrance of other particles, especially those in the form of aggregates (Fig. 8). Hence, when the surfaces of the microfibrils were completely covered with CB particles, the CB particles encounter hindrance in migration to PET phase, and so still stay in the matrix. These CB particles were almost in the form of aggregates. Nevertheless, the CB

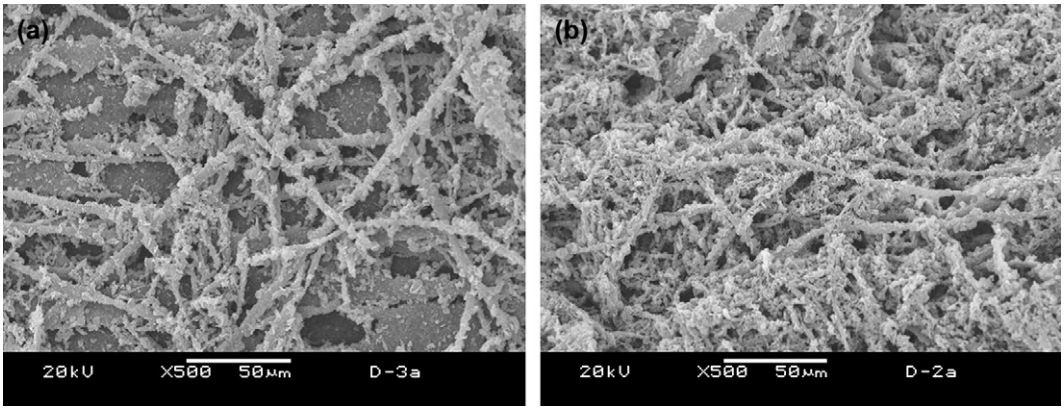

Fig. 7. SEM micrographs of the in situ microfibrillar i-CB/PET/PE composite with selectively locating CB in the surfaces of the microfibrils. The PE matrix was etched away by hot xylene for clear observation. The volume ratio of PET and PE is 1:3.2, the CB loading is 3.5 vol% and 7.2 vol% for (a) and (b), separately.

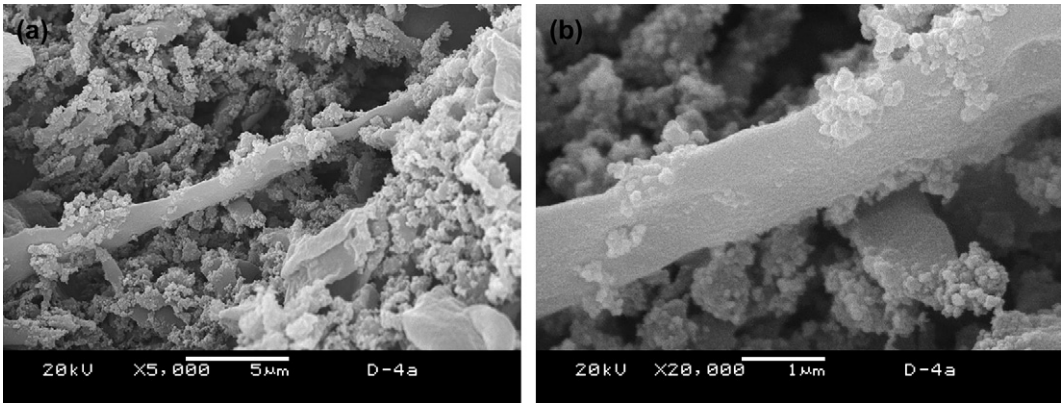

Fig. 8. SEM micrographs of the in situ microfibrillar i-CB/PET/PE composite with selectively locating CB in the surfaces of the microfibrils with low and high magnifications. The PE matrix was etched away by hot xylene for clear observation. The volume ratio of PET and PE is 1:3.2, the CB loading is 8.1 vol%.

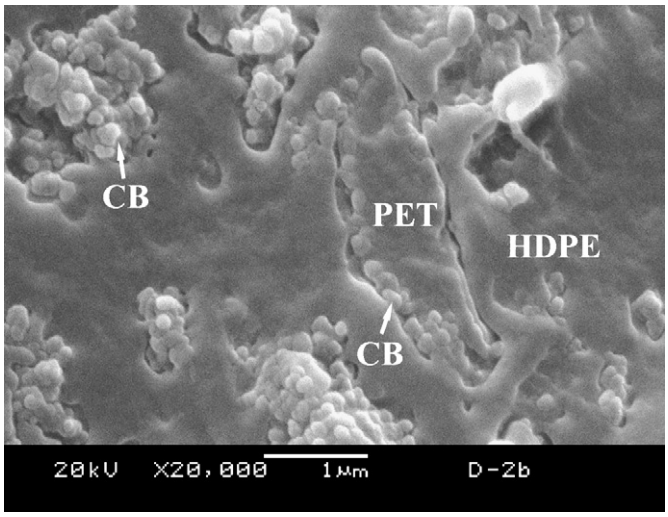

Fig. 9. SEM micrographs of the cryofractured surface of in situ microfibrillar i-CB/PET/PE composite with selectively locating CB in the surfaces of the PET microfibrils. The volume ratio of PET and PE is 1:3.2, and the CB loading is 4.93 vol%.

particles in the matrix can also help to build electrical networks together with the CB coated microfibrils. In this case, the matrix's morphology becomes rather complicated.

3.4. Electrical properties of the conductive in situ microfibrillar composite

Fig. 10 shows the correlation between the volume resistivity and CB loading for the microfibrillar i-CB/PET/PE composite. For comparison, the CB/PE composite is also shown in this figure. From these curves, the percolation can be estimated, which is ca. 3.8 vol% for the microfibrillar conductive composite, whereas ca. 6.8 vol% for d-CB/PET/PE and ca. 8.5 vol% for the common CB/PE conductive composites. A considerable reduction in percolation threshold has been successfully achieved using the present approach. At the CB percolation level, the resistivity of the microfibrillar composite is approximately reduced by 12 orders of magnitude. This assuredly demonstrates the superiority of the i-CB/PET/PE composite to the common conductive PET/PE composite. The low percolation threshold of i-CB/PET/PE was attributed to the fine contact of PET microfibrils with CB particles being distributed in their surfaces, but for the d-CB/PET/PE, PET phases were dispersed as many separate islands, though CB particles were distributed in the surfaces of PET phases, a perfect conductive network was hard to be constructed, and a high percolation threshold was obtained. In general, conductive CB/PE blends had a higher percolation threshold than both i-CB/PET/PE and d-CB/PET/PE.

To understand the conductive network as well as the electrical properties of the in situ microfibrillar i-CB/PET/PE, a conductive model is proposed as shown in Fig. 11. For simplicity, only several fibers are shown here. The inset A is the lateral face of a fiber, and B–B is the cross section of a fiber. The black points in the PE matrix denote the CB particles.

Regarding the formation of the conductive network in the i-CB/PET/PE composite, during compression molding, the local flow and diffusion of the melted PE made the CB particles coated microfibrils contact with each other and thus built a fine electrical network as shown in Fig. 11. Furthermore, the remaining CB particles in the matrix would quite possibly contribute to the transfer of the electrons, especially at a higher CB loading. When the CB loading was relatively low, CB particles were mostly located in the surfaces of microfibrils (Fig. 6(a)), and the conductive paths were, hence, formed mainly by the contacting of microfibrils, but their amount was limited due to the low CB content. If the CB particles scattered in the matrix and the CB coated microfibrils were not close enough, the tunneling conduction could also happen [52–54]. Although the two conduction modes coexisted, the resistivity of the in situ microfibrillar CB/PET/PE composite was still high because of the few conductive paths. In contrast, at a higher CB loading, the CB particles in the matrix

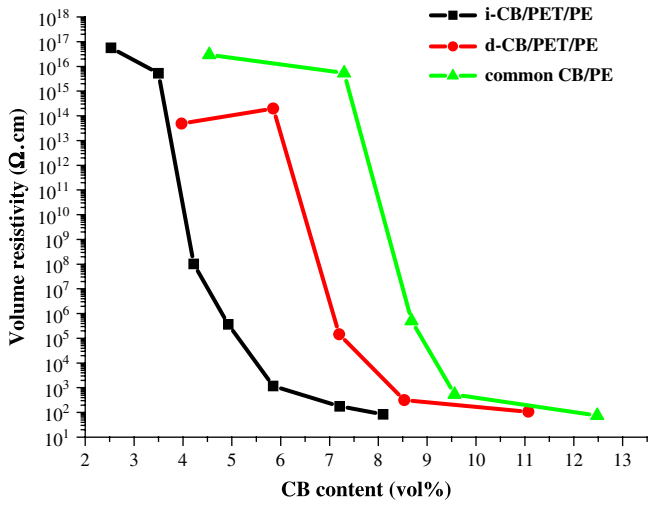

Fig. 10. Volume resistivity vs. CB content of i-CB/PET/PE composites, d-CB/PET/PE composites and common CB/PE composites.

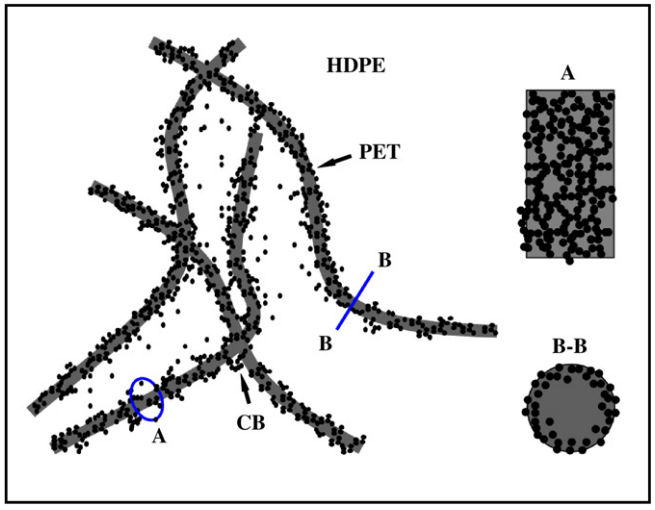

Fig. 11. Schematic illustration for the CB particles distribution and the electrical network in the in situ microfibrillar i-CB/PET/PE composite.

increased, the amount of conductive paths also increased by more conductive contact between CB particles and PET microfibrils so the resistivity of the blend was reduced. Therefore, by locating CB particles in the surfaces of the microfibrils, a more perfect conductive network than that in our previous work can be built by the contact of a few CB particles, and a high volume of CB particles is not required to fill the PET microfibrils to protrude some of them on the surfaces of the microfibrils to built a conductive network [30–34]. As a result, the impact of the maximum packing fraction Φ_{max} was removed, and a lower percolation threshold (about 3.8 vol%) than that in our previous work has been obtained.

Using the percolation concept, the electrical conductivity above the percolation threshold can be correlated as a universal law [46,55]:

$$\sigma = \sigma_0(\varphi - \varphi_c)^{-t} \tag{3}$$

where σ is the conductivity of the mixture with different filler contents, σ_0 is the conductivity of the filler, φ is the volume fraction of the filler, φ_c is the volume percolation concentration, and t is an exponent which fits the data and is used to predict the mechanism of electrical network.

The t value can be estimated from the slope of the line in a $\log(\varphi - \varphi_c)$ vs. $\log\sigma$ plot. Percolation threshold models depend on the t value. Generally, the t is about 1.1–1.3 for a two-dimensional system, while a higher value, in the range from 1.6 to 2.0 is for a three-dimensional system [46].

The $\log(\varphi - \varphi_c)$ vs. $\log\sigma$ plot for in situ microfibrillar i-CB/PET/PE composite exhibits a good linearity, as shown in Fig. 12. In Fig. 12, the t value of this composite is estimated according to Eq. (3), i.e., ca. 6.4. This value is very high, indicating that the system does not obey the universal percolation theory.

Recently, many investigations show that the practical conductive systems always deviate from the universal law [22,46].

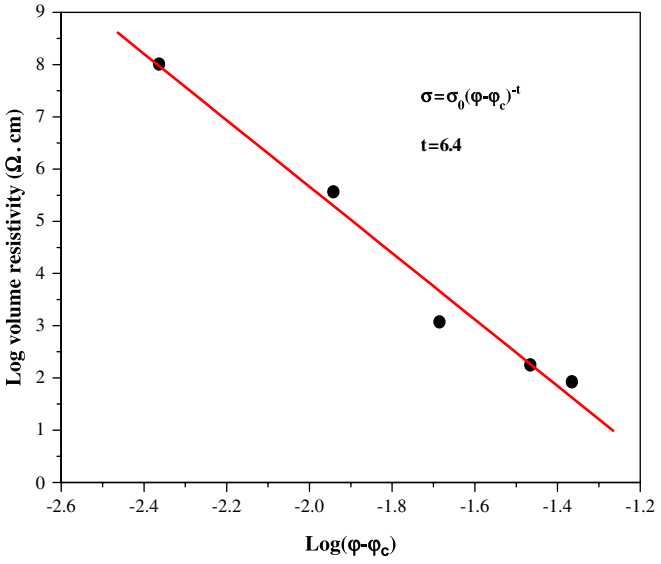

Fig. 12. Electrical conductivity as a function of excess concentration ($\varphi - \varphi_c$), for electrically conductive in situ microfibrillar i-CB/PET/PE composites.

Some researchers considered only single phase conductive composites to agree with the universal law well [46], while multi-phase conductive systems, especially multi-percolation systems, did not follow Eq. (3). Levon et al. studied the critical resistance exponent t of multiple-percolation CPC, and found that the exponent t was higher than that for the classical percolation theory [22,56,57]. Even in some single-percolation systems, the exponent t was higher than the universal value in some cases. In Foulger's study [58], the high exponent ($t = 3.1$) was attributed to the multiple percolation of the CB/HDPE blend. The separation of the crystalline and amorphous regions of the HDPE, coupled with the affinity of the carbon black to be preferentially located in the amorphous phase, could result in the composite exhibiting multiple-percolation characteristics.

However, for the microfibrillar i-CB/PET/PE composite, it is not a single-percolation system, and it cannot be considered as a double percolation system either (Fig. 11). Obviously, the reason of the high critical resistance exponent t cannot be attributed to a special single percolation or the multi-percolation. It must be determined by other factors, for example, the tunneling conduction effect is possibly an important element [52].

Balberg [53,54] confirmed the existence of the tunneling-percolation model in low structure CB (a DBP value of 43 $cm^3/100$ g) filled polymer composites. In their study, the exponent t of the CB/polyvinyl chloride (PVC) composite was about 6.4, which greatly deviates from the theoretical predictions of the universal model. This case was ultimately attributed to the nonrandom dispersion of the particles in these systems [53]. A higher critical resistance exponent $t = 7.75$ was reported in the FEF CB (a commercial CB product) filled styrene butadiene rubber (SBR) system. The electronic tunneling mechanism of conduction was effective [21]. The Ezquerra's study also gave a high exponent $t = 6.27$ of a graphite–PE blend [59].

For the in situ microfibrillar composite, though CB particles were located in the interfaces of the microfibrils selectively, there are still some CB particles (Fig. 11), usually in the form of aggregates, in the PE matrix. In other words, the distribution of CB is nonrandom and it is an important element to create a high critical resistance exponent t as reported [53,58]. Concerning the conductive mechanism, if the distance of two microfibrils is not close enough, the tunneling conduction possibly occurs. Tunneling conduction will also come into being between aggregates in the matrix, and this is another factor to make a high exponent t. The morphology of the microfibrils changes with increasing CB content, so does the morphology of the matrix. Consequently, the geometry of the electrical network becomes complex, understandably, the complexity can also make the system deviate from the theoretical prediction of the universal law.

In summary, the anisotropic distribution of CB particles, the tunneling conduction, the geometry of the electrical network, and the complex structure of the microfibrillar composite, etc. are likely to make the conducting composites deviate from the classical percolation theory, and a high value of the critical resistance exponent t was obtained.

4. Conclusions

All the factors affecting the distribution of CB particles in an immiscible blend, including interfacial tension, viscosity, chemical groups on the surface of CB particles and the processing order, are in favor of the migration of the CB particles from PE matrix to dispersed PET phases.

The migration of CB particles in the directly mixed PET/PE blend was examined. The morphological observation indicated that, depending on the mixing time, the CB particles gradually migrated from the PE matrix to the surfaces at first, and then to the center of the PET phases.

The electrically conductive in situ microfibrillar i-CB/PET/PE composite with the selective distribution of CB particles in the surfaces of the microfibrils was successfully fabricated. Well-defined PET microfibrils were generated in situ and a lot of CB particles were accumulated in the surfaces of the PET microfibrils. The percolation threshold of the in situ microfibrillar CPC was only ca. 3.8 vol%, showing a considerable decrease of percolation compared to that of the common CB/PE composite. The critical resistance exponent t of this composite was estimated, i.e., ca. 6.4. This value is very high, indicating that the system does not obey the prediction of the universal percolation theory. The anisotropic distribution of CB particles and the tunneling conduction can be the possible origin of the high t value.

Acknowledgements

The authors gratefully acknowledge the financial support of this work by the Nature Science Foundation of China (Contract Number: 50573049), and Programs for New Century Excellent Talents in University (Grant Number: NCET-04-0871) and Innovative Research Team in University. Thanks are also given to Mr. Zhu Li from Analytical & Testing Center of Sichuan University for his help in the SEM observation.

References

[1] Sumita M, Sakata K, Asai S, Miyasaka K, Nakagawa H. Polym Bull 1991;25:265–71.
[2] Thongruang W, Baik CM, Spontak R. J Polym Sci Part B Polym Phys 2002;40:1013–23.
[3] Kohjiya S, Katoh A, Suda T, Shimanuki J, Ikeda Y. Polymer 2006;47:3298–301.
[4] Yui H, Wu GZ, Sano H, Sumita M, Kino K. Polymer 2006;47:3599–608.
[5] Jdger KM, Eggen SS. Polymer 2004;45:7681–92.
[6] Gojny FH, Wichmann MHG, Fiedler B, Kinloch IA, Bauhofer W, Windle AH, et al. Polymer 2006;47:2036–45.
[7] Meincke M, Kaempfer D, Weickmann H, Friedrich H, Vathauer M, Warth H. Polymer 2004;45:739–48.
[8] Wang WP, Pan CY. Polymer 2004;45:3987–95.
[9] Song Y, Pan Y, Zheng Q, Yi XS. J Polym Sci Part B Polym Phys 2000;38:1756–63.
[10] Breeze AJ, Carter SA, Alers GB, Heaney MB. Appl Phys Lett 2000;76:592–4.
[11] Bloor D, Donnelly K, Hands PJ, Laughlin P, Lussey D. J Phys D Appl Phys 2005;38:2851–60.
[12] Thongruang W, Spontak RJ, Balik CM. Polymer 2002;43:2279–86.
[13] Di W, Zhang G. J Mater Sci 2004;39:695–7.
[14] Schueler R, Petermann J, Schulte K, Wentzel HP. J Appl Polym Sci 1997;63:1741–6.
[15] Segal E, Tchoudakov R, Narkis M, Siegmann A. J Mater Sci 2004;39:5673–82.
[16] Tantawy FE, Kamada K, Ohnabe H. Polym Int 2002;51:635–46.
[17] Dong XM, Fu RW, Zhang MQ, Zhang B, Rong MZ. Carbon 2004;42:2551–9.
[18] Breuer O, Tchoudakov R, Narkis M, Siegmann A. J Appl Polym Sci 1997;64:1097–106.
[19] Tchoudakov R, Breuer O, Narkis M. Polym Eng Sci 1996;36:1336–46.
[20] Chen Z, Brokken-Zijp JCM, Michels MAJ. J Polym Sci Part B Polym Phys 2006;44:33–47.
[21] Karasek L, Meissner B, Asai S, Sumita M. Polym J 1996;28:121–6.
[22] Levon K, Margolina A, Patashinsky AZ. Macromolecules 1993;26:4061–3.
[23] Hu JW, Li MW, Zhang MQ, Xiao DS, Cheng GS, Rong MZ. Macromol Rapid Commun 2003;24:889–93.
[24] Tai XY, Wu GZ, Tominaga Y, Asai S, Sumita M. J Polym Sci Part B Polym Phys 2005;43:184–9.
[25] Foulger SH. J Polym Sci Part B Polym Phys 1999;37:1899–910.
[26] Narkis M, Lidor G, Vaxman A, Zuri L. J Electrostat 1999;47:201–14.
[27] Gubbels F, Jérôme R, Teyssié P, Vanlathem E, Deltour R, Calderone A, et al. Macromolecules 1994;27:1972–4.
[28] Gubbels F, Blacher S, Vanlathem E, Jérôme R, Deltour R, Brouers F, et al. Macromolecules 1995;28:1559–66.
[29] Prasse T, Fandin L, Bauhofer W. Appl Phys Lett 1998;72:2903–5.
[30] Li ZM, Xu XB, Lu A, Shen KZ, Huang R, Yang MB. Carbon 2004;42:428–32.
[31] Xu XB, Li ZM, Yu RZ, Lu A, Yang MB, Huang R. Macromol Mater Eng 2004;289:568–75.
[32] Xu XB, Li ZM, Yang MB, Jiang S, Huang R. Carbon 2005;43:1479–87.
[33] Li ZM, Li LB, Shen KZ, Yang MB, Huang R. Polymer 2005;46:5358–67.
[34] Xu XB, Li ZM, Dai K, Yang MB. Appl Phys Lett 2006;89:032105.
[35] Wu GZ, Asai S, Sumita M. Macromolecules 2002;35:945–51.
[36] Asai S, Sakata K, Sumita M, Miyasaka K. Polym J 1992;24:415–20.
[37] Wu S. Polymer interface and adhesion. New York: Marcel Dekker; 1982.
[38] Feng J, Chan CM, Li JX. Polym Eng Sci 2003;43:1058–63.
[39] Persson AL, Bertilsson H. Polymer 1998;39:5633–42.
[40] Huang JC. Adv Polym Technol 2002;21:299–313.
[41] Yoon HG, Kwon KW, Nagata K, Takahashi K. Carbon 2004;42:1877–9.
[42] Le HH, Prodanova I, Ilisch S, Radusch HJ. Rubber Chem Technol 2004;77:815–29.
[43] Sirisinha C, Prayoonchatphan N. J Appl Polym Sci 2001;81:3198–203.
[44] Favis BD, Willis JM. J Polym Sci Part B Polym Phys 1990;28:2259–69.
[45] Plochocki AP, Dagli SS, Andrews RD. Polym Eng Sci 1990;30:741–52.
[46] Babinec SJ, Mussell RD, Lundgard RL, Cieslinski R. Adv Mater 2000;12:1823–34.
[47] Min K, White JL, Fellers JF. Polym Eng Sci 1984;24:1327–36.
[48] Hobbs JK. Polymer 2006;47:5566–73.
[49] Verhoyen O, Dupret F, Legras R. Polym Eng Sci 1998;38:1594–610.
[50] Harpaz IM, Narkis M. J Polym Sci Part B Polym Phys 2001;39:1415–28.
[51] Xi Y, Ishikawa H, Bin YZ, Matsuo M. Carbon 2004;42:1699–706.
[52] Balberg I. Phys Rev Lett 1987;59:1305–8.
[53] Rubin Z, Sunshine SA, Heaney MB, Bloom I, Balberg I. Phys Rev B 1999;59:12196–9.
[54] Balberg I. Carbon 2002;40:139–43.
[55] Kirkpatrick S. Rev Mod Phys 1973;45:574–88.
[56] Wang Y, Rubner MF. Macromolecules 1992;25:3284–90.
[57] Inaba N, Sato K, Suzuki S, Haehimoto T. Macromolecules 1989;19:1690–5.
[58] Foulger SH. J Appl Polym Sci 1999;72:1573–82.
[59] Ezquerra TA, Kulescza M, Cruz CS, Balta-Calleja FJ. Adv Mater 1990;2:597–600.